THE JOURNAL OF PHYSICAL CHEMISTRY B

ARTICLE

pubs.acs.org/JPCB

Computer Simulations of Gas Diffusion in Polystyrene−C_{60} Fullerene Nanocomposites Using Trajectory Extending Kinetic Monte Carlo Method

Ben Hanson, Victor Pryamitsyn, and Venkat Ganesan*

Department of Chemical Engineering, University of Texas at Austin, Austin, Texas 78712, United States

ABSTRACT: The effects of nanoparticles on the rates of gas diffusion through glassy polymers were studied by a combination of molecular dynamics and kinetic Monte Carlo techniques designed to overcome the computational limitations in obtaining long-time trajectories in the diffusive regime of gas molecules in glassy polymer systems. Using such a methodology, we studied the effect of fullerene nanoparticles upon the diffusivities of N_2 and CO_2 in a polystyrene matrix. The addition of nanoparticles was found to cause a lowering of the diffusion coefficients of both N_2 and CO_2. However, the magnitudes of this lowering and their volume fraction dependencies are seen to depend explicitly on the nature of the penetrant and temperature. We discuss the possible physical mechanisms underlying such behavior.

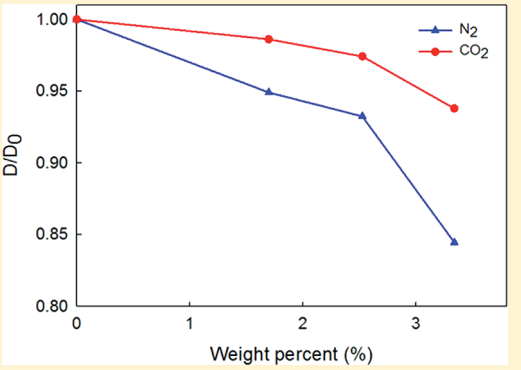

I. INTRODUCTION

Polymeric materials with controlled permeability properties are used widely in packaging,[1−4] industrial gas separations,[5−8] biomedical engineering,[9] and energy storage applications.[10−15] The fundamental parameters characterizing membrane separation performance are its permeability coefficient P, and its selectivity relative to different components. In many separation applications, polymers with both high permeability and high selectivity are desired. Higher permeability decreases the amount of membrane area required to treat a given amount of gas, thereby decreasing the cost of membrane units. On the other hand, higher selectivity results in higher purity of the desired product gas.[16]

Systematic measurements of gas separation properties of polymer membranes have been effected in an effort to design polymers that possess the above holy grail of high permeability/high selectivity combination. As an outcome of such studies, it has, however, become clear that there is a rather general tradeoff between permeability and selectivity of polymer membranes. Polymers that were usually more permeable were generally less selective and vice versa. Recently, however, heterogeneous materials comprising a polymer matrix and inorganic dispersed phases have attracted interest as a platform to potentially realize the above desired combination of properties. Traditionally, transport properties in polymer/inorganic heterophase materials exhibit permeability behavior reflecting the transport properties of the individual phases.[17] Because the inorganic phases are impermeable, this usually means a reduction in the overall permeability of the polymer membrane. However, recent experiments have pointed to exceptions to such behaviors. For example, poly(4-methyl-2-pentyne) (PMP) filled with 25 vol % fumed silica (FS) exhibited N_2 permeability coefficients approximately 3 times higher than those of unfilled PMP.[18] In another study, the propylene/propane selectivity increased from near unity in a poly(ethylene-*co*-propylene) film to 180 in a poly(ethylene-*co*-propylene) film containing 50 wt % Ag nanoparticles and 0.8 wt % *p*-benzoquinone.[19] These studies have led to the realization that incorporating small, nanoscopic inorganic fillers in polymers may alter the gas transport properties in such a way that the properties of the resulting composite materials are far superior to the properties that can be obtained from pure polymers alone.

Motivated by the above experiments, there have been several theoretical investigations modeling the barrier properties of polymer nanocomposite (PNC) membranes. Of fundamental interest to these studies are the mechanistic underpinnings of the barrier properties of polymer nanocomposites, and whether there are factors that render them to be different from the trends expected for polymer composites (i.e., polymers containing large filler particles). Continuum mechanical composite theories for the effective diffusivity of a two-phase dispersed system considers only the presence of two phases, viz., the particle phase and the medium (polymer phase) with their specific properties.[20−24] Because the particles in the membranes are usually nonporous, the trends from such models can only predict a *decrease* in membrane permeability upon addition of fillers. To account for filler-induced modification of polymer properties, some researchers have probed the role of modified polymer interfacial properties by the use of three-phase models that posit the presence of three

Received: September 26, 2011
Revised: November 18, 2011
Published: November 29, 2011

well-defined phases, viz., the particle, polymer medium, and an "interfacial region" that is assumed to have its own physical properties.[25−29] Using such models, these studies have demonstrated that for appropriate choice of interfacial parameters (i.e., the size of the interfacial zones and the transport coefficients in such regions) one can potentially offset the obstructive role of the particles and lead to enhancements in the permeability of penetrants.

In a recent article,[30] we used coarse-grained simulations to critically confront the above models and also examine the role of polymer segmental dynamics upon the transport properties of polymer−nanoparticle mixtures. Our results indicated that the penetrant transport properties are dominated by the "filler" effect, in which the particles act as obstructions for the penetrant diffusion. Interfacial effects, which are driven by the polymer−particle interactions, were shown to play a role, but their impact was demonstrated to be less important relative to the filler effect. A second outcome of our work was a demonstration that the matrix dynamics on the scale of the penetrant size plays an important role in determining the overall transport properties of the PNC. For nanoparticle systems, such effects are shown to lead to significant deviations from continuum mechanical theories for the effective properties of particulate dispersions.

Although the above study provided new insights regarding the transport properties of polymer nanocomposites, due to the coarse-grained nature of the simulation formalism adopted, the shortest units of length and time scale in such models corresponded to that of polymer segments. Consequently, our model and results presented therein were most suited for describing penetrant motions which either are coupled to or happen at the scale of the segmental dynamics of the polymers—features representative of the motions of large probe molecules as well as ions arising from alkali metal salts. In contrast, the dynamics of small gas molecules (such as H_2, O_2, CO_2, etc.) in glassy polymer membranes have been shown to be decoupled from the segmental motions of the polymer matrix and to be instead dependent only on the high frequency vibrational motions of the polymer chains. Accounting for such effects in simulations requires atomistically realistic models and was beyond the focus of our earlier article. Consequently, the mechanisms underlying the transport properties of small gas molecules in polymer nanocomposites are as-yet unresolved.

In this article, we complement the results of our coarse-grained simulations by presenting atomistically realistic simulations of gas diffusion in polymer nanocomposite matrices. To overcome the computational challenges accompanying such an effort, we employ a recently proposed trajectory-extending kinetic Monte Carlo scheme that allows us to track the long-time diffusion of gases through polymers ranging in conditions from rubbery to glassy states. As a model system, we consider nanocomposites of polystyrene and fullerene nanoparticles and study the diffusion properties of CO_2 and N_2 gases as a function of the fullerene loading. Such a system is attractive for computer simulations, due to the availability of appropriate force fields for the different components, as well as due to the existence of experimental results that have probed the mechanical and barrier properties of such nanocomposites. Explicitly, Wong et al.[31] used various spectroscopy methods to study the impact of fullerene nanoparticles upon the dynamics and glass formation of polystyrene matrices. They found that the addition of a low concentration of nanoparticles (<4% by weight) hinders segmental motion in the polymer, resulting in an increase in the glass transition temperature. Additionally, they observed that high nanoparticle loading resulted in agglomeration of nanoparticles. The larger groups of aggregated particles had a lesser effect on the glass transition temperature of the polymer. An experimental study by Polotskya et al.[32] examined the effect of fullerene nanoparticles on oxygen and nitrogen gas diffusion through polystyrene. It was observed that the addition of up to 3 wt % nanoparticles resulted in a decrease in the diffusivity of both gas types. As with the study by Wong, they observed some aggregation of the fullerene particles at the higher weight percentages.

The rest of this article is arranged as follows: In section II, we briefly discuss the background on the simulation challenges and the strategies pursued for simulating gas diffusion through glassy polymer matrices. Subsequently, we present an overview of the methodology adopted in our work. In section III, we present the results and a discussion of the underlying mechanisms of the gas diffusion. A brief summary and overall conclusions drawn from this work follows in section IV.

II. SIMULATION METHODOLOGY

A. Trajectory Extending Kinetic Monte Carlo Simulations. Computer simulations of the diffusivity D, of gas molecules in glassy polymer matrices proves an especially challenging task.[33] Molecular dynamics simulations, a technique that is typically used for predicting the diffusivity of molecules, falls short of the relevant time scales required for characterizing penetrant diffusivities in glassy polymer matrices. The are two main reasons for this shortcoming. (i) Diffusivity values are extremely small for penetrants in glassy polymers. Indeed, penetrant diffusivities of the order of 10^{-9} cm^2 s^{-1} in glassy polymer matrices are not uncommon. This would imply that the penetrants hardly move at all within any reasonable time frame of a molecular dynamics simulation! (ii) Diffusive transport in glassy polymers is believed to occur through a hopping mechanism. In such a case, the penetrant motion consists of "rare hops" interspersed with long time periods of immobility. A study by Han and Boyd[34] used molecular dynamics simulations to examine the diffusion of methane in polystyrene and observed that penetrant motion by the hopping motion was not limited to systems below or even near the glass transition temperature. They noted that the onset of this motion occurred well above the glass transition temperature with the frequency and length of hops decreasing with decreasing temperature. This hopping motion is not limited to this specific system and has been observed for a number of different penetrants and polymers.[35−37] Achieving quantitative predictions for the diffusivity requires averaging over many such hops, which is infeasible in traditional MD simulations.[33]

The above issues have, however, been surmounted by creative strategies primarily devised by the groups of Suter, Theodorou, and their co-workers.[38−43] These strategies involve atomistic simulations on smaller systems to identify both the states where the penetrant spends most of its time and the reaction paths along which transitions between the neighboring states take place. The rate constants for such reaction paths are then computed using sophisticated implementations of transition state theory as applied to the motion of the penetrant molecules. The distribution of such sorption states, their connectivities, and the rate constants are then used to generate a network of sites on a much larger system representative of the membrane. Such a network is then used in a coarse-grained kinetic Monte Carlo (KMC) simulation to deduce the overall diffusivity of the penetrant molecules.[40] Together, the above developments have

rendered viable the semiquantitative prediction of barrier properties of *pure* polymer membranes starting from an atomistically realistic description of the penetrant-polymer system.

In this work, we adopt a recently proposed trajectory extending Monte Carlo scheme[44,45] as a methodology to overcome the above-discussed computational challenges. This technique is less accurate than the more sophisticated techniques proposed by Suter, Theodorou, and co-workers. On the other hand, because we are only interested in the *mechanisms* underlying gas diffusivities of polymer nanocomposites, we accommodate this loss in accuracy in lieu of the simplicity of implementation of such a procedure. Because earlier articles have provided a detailed overview of this methodology, we restrict our discussion to just an overview of the main details. In short, the idea behind this simulation technique is to use stored configurations of the polymer−penetrant systems from MD simulations over short time scales (but still long enough for the penetrant molecules to explore a significant part of the simulation system) to extend the time range over which penetrant mean-square displacements are calculated. To implement this idea, the methodology invokes a MD simulation of the polymer system containing a number of gas molecules over a span of time. Care must be given to simulate the system a sufficient amount of time to sample continuous gas diffusion paths through the simulation box. The position of the gas molecules are then translated onto positions on a box with an evenly spaced grid, and the occupancy of such a grid is recorded. This procedure is repeated at the end of each MD simulation output step (of fixed time span). Using the occupation statistics, changes in gas positions between the initial and subsequent positions are recorded and used to create a matrix of the probability of motion by the gas molecule. The probability that the particle has remained within the same coordinate box is also recorded to represent the times in which the gas molecule is trapped and is not able to move.

The above probability matrix is used as the basis of the trajectory extending Monte Carlo simulations. In such a situation, a penetrant representative of the gas molecule is inserted to the simulation lattice. The initial position must be correlated to a position that the gas has occupied in the molecular dynamics simulation. A random number is generated and compared to the probability of motion for the grid box. The position is updated and the motion of the particle is tracked to generate a long time trajectory for the penetrant with relatively low computational resources. This procedure is repeated and the resulting trajectories can be used to calculate the mean square displacement of the representative penetrant. It is important to note that the diffusivity can be dependent on the size of the boxes in the probability grid and must be fine-tuned. The mean square displacement for gas calculated from the short atomistic simulations is used as a reference point and the box size adjusted until the values produced by the trajectory extending kinetic Monte Carlo scheme match those found from the atomistic simulations. This process is explained in greater detail below in section III. The mean-squared displacement of the penetrant is then used to calculate the diffusion coefficient as

$$D = \frac{1}{6N}\lim_{t\to\infty}\frac{\mathrm{d}}{\mathrm{d}t}\left\langle \sum_{N}^{i}[r_i(t) - r_i(0)]^2\right\rangle$$

where D is the diffusion coefficient, r_i is the center-of-mass position of the gas molecule, N is the total number of gas molecules inserted, and t is the time.

B. Simulation Details. Fully atomistic MD simulations were performed for a melt of 4 chains of pure polystyrene of 200 repeat units utilizing the MD simulation package LAMMPS.[46] The Lennard-Jones and electrostatic interactions in real space were truncated at 8.0 Å. Simulations were performed in the *NPT* ensemble at 1 atm and 250−500 K utilizing the Nose−Hoover[47,48] thermostat and Andersen−Hoover barostat.[49] We employed the transferable potentials for phase equilibria (TraPPE) united atom force field for the polystyrene,[50] nitrogen, and oxygen[51] interactions. The Dreiding force field was used to model the C_{60} fullerene nanoparticles.[52] Parameters for unlike nonbonded interactions were calculated using the Lorentz−Berthelot mixing rules.[53]

The system was initially formed with 4 polystyrene chains of 200 monomers using Accelrys Materials Studio[54] and simulated at an elevated temperature to accelerate entanglement, relaxation, and equilibration. Systems with C_{60} nanoparticle weight percentages of 1.7−3.34% were also created at this point. The melt was determined to have reached a state equilibrium when the total energy of the system did not appreciably decrease for approximately 2 ns. The systems are incrementally quenched with lowering the temperature approximately 25 K per 2−4 ns. Eleven individual systems were created from 250 to 500 K at 25 K intervals. Following the methodology found in Yampol'skii et al.,[16] an isothermal compression is performed on the simulation box. Each system is freely simulated at the desired temperature for an additional 4 ns to further ensure proper relaxation. After this procedure is completed, 50 gas molecules are randomly inserted into the polymer matrix. The system is allowed to run with the gas freely diffusing throughout the simulation box. Subsequently, the trajectory extending kinetic Monte Carlo scheme described in the preceding section was used to probe the diffusivities of the gaseous penetrants.

III. RESULTS AND DISCUSSION

Prior to presenting our results for the diffusivity of gaseous penetrants in polymer nanocomposite matrices, we briefly summarize the main findings of our earlier work that used coarse-grained simulations to study the transport of ions and large probes in polymer matrices. Explicitly, for such situations we found that (i) overall penetrant diffusivities are dominated by the "filler" effect, in which the particles act only as obstructions for the penetrant diffusion. As a consequence, the overall penetrant diffusivities (at a specified temperature) were reduced upon addition of particles. (ii) The penetrant diffusivities were shown to be significantly influenced by the changes in the bulk conditions (densities and free volumes) of the polymer matrix that were induced by the addition of nanoparticles. (iii) There was a nontrivial interplay between polymer segmental dynamics and the obstructional role of the particles, which led to significant deviations from continuum mechanical predictions quantifying the "filler" effect of the particles.

Motivated by the above considerations, the results and analysis presented in this section seek to address the following issues: (i) the impact of "filler" effect upon the transport of penetrants; (ii) the role of polymer dynamics upon penetrant transport in nanocomposites; (iii) the influence of changes in bulk conditions upon the transport properties of the penetrants.

A. Validating the Trajectory Extending Kinetic Monte Carlo Method. At the outset, we present a short discussion regarding the implementation of the trajectory extending the

dx.doi.org/10.1021/jp209294t |J. Phys. Chem. B 2012, 116, 95–103

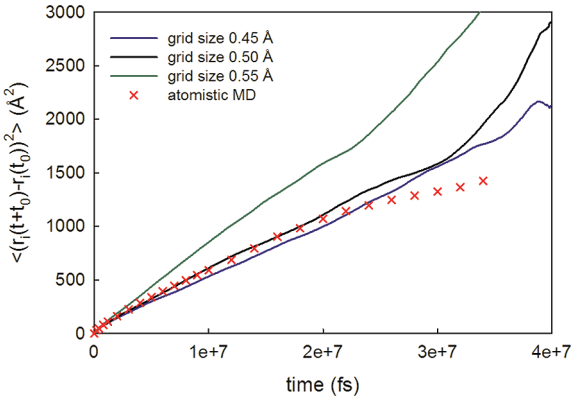

Figure 1. Fitting of the TEKMC displacement to the atomistic results at 300 K and 2.53 wt % nanoparticle system.

kinetic Monte Carlo (TEKMC) scheme. In the earlier articles by Neyertz and Brown,[44] it has been noted that the results obtained on the basis of the TEKMC trajectories are sensitive to two parameters: (i) the output frequency of the atomistic MD simulation snapshots, which constitute the starting point for construction of the probability matrix of the MD simulation, and (ii) the size of the individual grid boxes used to construct the probability statistics for penetrant motions. When the output frequency is chosen, a balance must be found between computational speed and resolution of the gas molecule trajectory. Capturing the simulation data too often can become very memory intensive and necessitates a large amount of time and computational resources to generate the probability matrix. Additionally, the data may not capture jumps frequently enough to produce a matrix with a sufficient statistics of movement between trapped regimes. If the output frequency is too long, the gas molecules may have moved a distance greater than half of the simulation cell length, resulting in an underestimation of the gas molecule motion. It is also important to perform the atomistic simulation long enough to generate a high percentage of connectivity between visited cells. This is essential due to the fact that the TEKMC diffusivity of a particle in an unlinked channel is essentially zero.

The size of the probability grid can also greatly influence the resulting trajectory. Ideally, the grid size should reflect the movement of the gas molecule within the trapped regime. If the grid size is too small, it will not reflect the connectivity of the trapped areas and lead to lower diffusivities. On the other hand, if the grid size is too large, the connectivity is overestimated, which leads to too high diffusion. The grid size is adjusted to fit the mean square displacement calculated from kinetic Monte Carlo to the mean-squared displacement values calculated for a 4 ns atomistic simulation. It was found that the temperature and weight percent of nanoparticles in the system has a large influence on the grid size necessitating a new fit at each condition. It can be seen from Figure 1 the ability if the TEKMC to reproduce the atomistic values and the influence grid size has on the resulting displacements. It should be noted that the divergence of the TEKMC and atomistic displacements above 2e+7 fs is due to poor statistics and does not have an influence on the grid fitting.

Experimental results report that a polystyrene chain of 100 monomers has a N_2 diffusivity of 6.0×10^{-8} cm^2 s^{-1}, whereas using the TEKMC method on our system of polystyrene chains of 200 monomers at the same temperature and pressure gave calculated diffusivities of 2.38×10^{-8} cm^2 s^{-1}. Although the comparison is not exact, we feel that this methodology is able to reasonably reproduce experimental data[55] and use it as a starting point for analyzing the mechanisms underlying penetrant diffusivities in polymer nanocomposites.

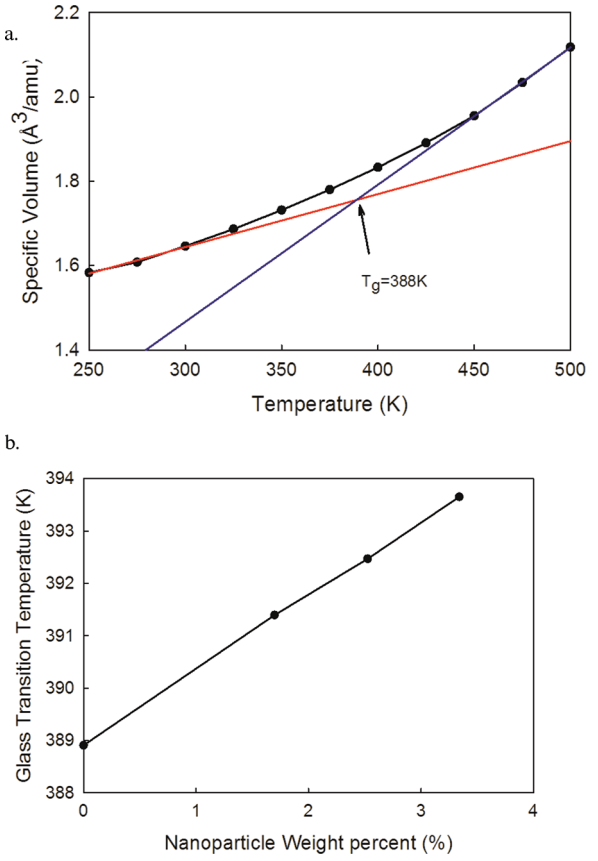

Figure 2. (a) Specific volume vs temperature for the pure PS matrix. (b) Glass transition temperature as a function of nanoparticle weight percentage.

B. Impact of Nanoparticles upon the Glass Transition Temperature of Polymer Matrix. As a preliminary step to probing the impact of polymer matrix dynamics upon the transport properties of penetrants, we determined the changes in the glass transition temperature of the polymer matrix due to the addition of nanoparticles. This was accomplished by calculating the density of the systems at a range of temperatures above and below the theorized glass transition temperature. Results were analyzed in terms of the changes in the specific volume as a function of temperatures. A linear fit is calculated for the specific volume at the highest and lowest temperatures using the least-squares methodology. The temperature at the intersection of the two fitted lines is taken to represent the glass transition temperature of the system (Figure 2a). It should be noted that the resulting specific volume values are not extensive enough to see the dramatic shift usually seen in the experiments at the glass transition temperature; however, the curves are still seen to provide a useful estimate for T_g.

The resulting glass transition temperatures are displayed as a function of nanoparticle loading in Figure 2b. It can be seen that the addition of the nanoparticles results in an increase of the glass transition temperature. These trends and the quantitative values of the shifts are consistent with the experimental results of Wong et al.,[31] in which such behavior was rationalized by evidence

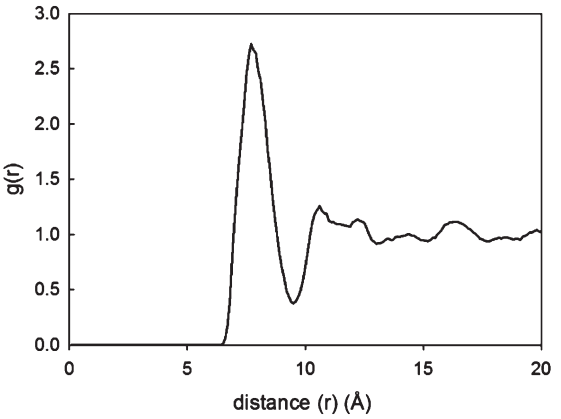

Figure 3. Radial distribution function calculated between polymer monomers and the nanoparticle center of mass.

which showed that the C_{60} nanoparticles hinder the collective segmental motions of PS matrix. At a physical level, such effects can be rationalized by noting that the PS matrices exhibit (weak) attractive interactions with the C_{60} particles. The latter is expected to lead to a denser packing near the surface of the particles and a corresponding increase in the T_g of the nanocomposite.[56]

To validate the above hypothesis regarding the impact of nanoparticles upon the polymer densities (and its consequent impact upon T_g), we probed the densities of the polymer monomers near the particle surfaces. These results are displayed in Figure 3 at a temperature of 250 K, where a clear increase in the density of the polymer monomers near the surface of the particle.

C. Influence of Temperature and Nanoparticles upon Penetrant Trajectories. At the outset, we discuss the characteristics of the trajectories of the penetrant motion and the influence of temperature and nanoparticle loading upon such features. Parts a and b of Figure 4 depict the trajectories of the CO_2 penetrant molecule in the pure PS matrix at temperatures above and below the glass transition temperature. It is seen that at the higher temperature, the penetrant trajectory exhibits a behavior characteristic of normal or Fickian diffusion. In contrast, below T_g, the penetrant's motion is more characteristic of a hopping mechanism, in which the penetrant spends a substantial fraction of the time trapped in the polymer voids interspersed by jumps to nearby voids. The jump mechanism is highlighted by the individual square displacement (Figure 4c). Trapped molecules oscillate within the same site with amplitude of approximately 0−3 Å, and are punctuated by larger, infrequent jumps back and forth between sites. Such behavior is qualitatively consistent with the results of prior studies which have used molecular dynamics simulations to quantify the diffusivity of penetrants in glassy matrices.[34,36,45,57−61]

What is the influence of nanoparticles upon the above-discussed trajectories? To answer this question, we take recourse to the literature on heterogeneous dynamics in glassy media and borrow a more quantitative measure of the penetrant trajectory referred to as the non-Gaussian parameter $\alpha(t)$. The latter is defined as

$$\alpha = \frac{3[r_i(t) - r_i(0)]^4}{5([r_i(t) - r_i(0)]^2[r_i(t) - r_i(0)]^2)} - 1$$

and serves to quantify the deviations from the normal diffusive behavior. In Figure 5 we display $\alpha(t)$ at a temperature of 250 K for different particle concentrations.

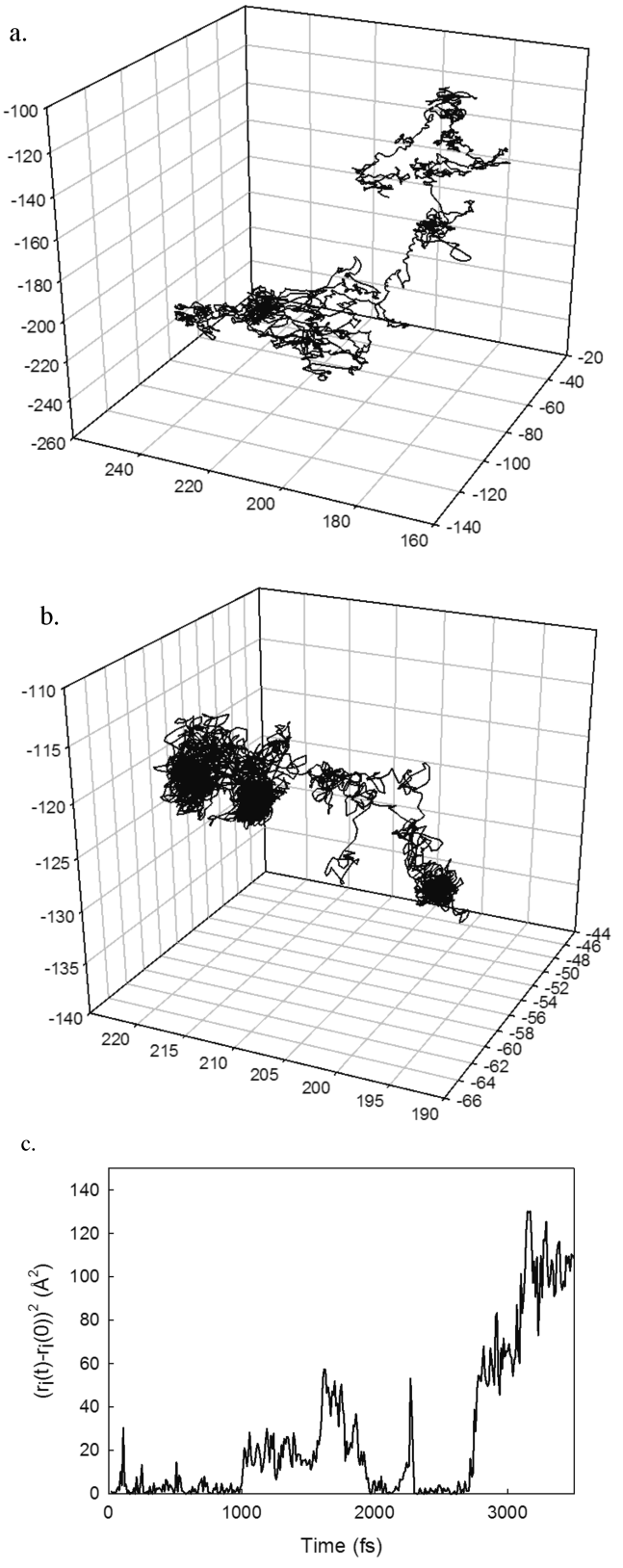

Figure 4. Penetrant (N_2) trajectories at (a) 500 K and (b) 250 K with the axes indicating x, y, and z positions within the simulation box. (c) Displacements of a single N_2 molecule.

We observe that with increased particle loadings, the peaks in $\alpha(t)$ are slightly enhanced, which is indicative of more pronounced

dx.doi.org/10.1021/jp209294t |J. Phys. Chem. B 2012, 116, 95–103

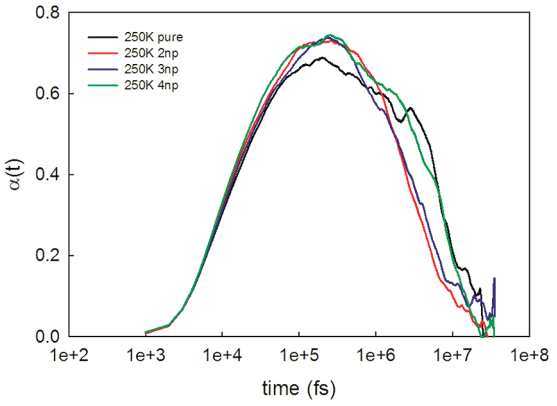

Figure 5. $\alpha(t)$ values displayed as a function of simulation time.

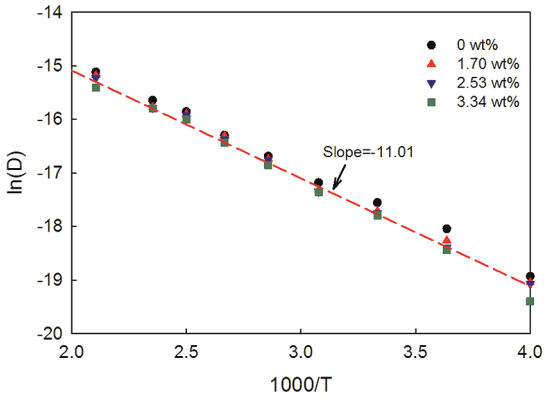

Figure 6. Arrhenius plot of diffusion of N_2.

heterogeneities governing the motion of the penetrants. We note that such behavior is qualitatively consistent with the influence of the particles upon the T_g of the polymer. Indeed, the trends seen in the context of Figure 2b were argued to be a consequence of the densification of the polymer segments near the particle surfaces and were validated by the results of Figure 3. Such local densification is expected to lead to a corresponding decrease in the size of void spaces, and in turn, an enhanced propensity for the penetrants to get trapped and increase the heterogeneities in their motion.

In summary, the results presented in this section confirm that the penetrant motion exhibits qualitatively different features at temperatures above and below the glass transition. Moreover, nanoparticles are seen to influence (albeit, only slightly) such characteristics by enhancing the heterogeneities accompanying the penetrant motion. In the following section, we examine the impact of such characteristics upon the long-time diffusivities of penetrants.

D. Influence of Temperature and Nanoparticles upon Penetrant Diffusivities: Results. The trajectory extending kinetic Monte Carlo procedure mentioned above was performed to obtain the gas diffusion rates of both CO_2 and N_2 penetrants over the studied range of temperatures (Figures 6 and 7). A number of studies have suggested that the diffusion coefficients of gases D can be fit to an Arrhenius form:

$$D = D_0 \exp(-E_d/RT)$$

where E_d denotes a characteristic activation energy, T the temperature, and R represents the gas constant. From the results displayed, it is evident that the diffusivities of N_2 are systematically higher than that of CO_2, a trend that can be rationalized as a consequence of the larger size of the CO_2 penetrants. More interestingly, it is seen that the results for N_2 follow a linear relationship between $\ln(D)$ and $1/T$ over the entire range of temperature studied. In contrast, the temperature dependence of CO_2 displays a non-Arrhenius behavior that roughly resembles a combination of two Arrhenius behaviors with two different slopes (albeit, close in magnitude) with a break at a temperature close to the glass transition temperature of the matrix.

We note that the qualitative trends noted for the diffusion of CO_2 and N_2 molecules in the pure polymer matrix are in agreement with a recent article that reported the temperature diffusion coefficients of N_2, CO_2 (and other gases) in polystyrene matrices.[36] Explicitly, the authors demonstrated that the diffusion coefficients of smaller gases like argon and nitrogen exhibited an Arrhenius behavior over the entire temperature range. In contrast, the diffusion coefficients of larger molecules such as CO_2, methane, and propane showed different slopes above and below the glass transition temperature. We do note that the quantitative values of the diffusivities of this article are lower than reported, which is likely a consequence of the use of the more approximate method employed in this article to compute the diffusivities.

With increased particle loading, it is seen that the diffusivities of the penetrants are systematically lowered. However, the qualitative features of the temperature dependencies are seen to be maintained at the different particle loads. To illustrate more clearly the influence of nanoparticles upon the diffusion coefficients of gas molecules, in Figure 8a,b we display at three different temperatures (400, 350, and 300 K) the diffusion coefficients of N_2 and CO_2 as a function of particle loading. It is evident that addition of nanoparticles leads to a reduction in the diffusion coefficient of the gas molecules. Such trends are broadly consistent with the physical picture wherein the fillers act as obstructions to the transport of penetrants (termed earlier in this article as the filler effect).

Despite the qualitative conformance of the above results to the "filler" role of particles, we note several nontrivial trends: Explicitly, we note the particle loading dependencies of the diffusion coefficients are not the same for CO_2 and N_2. Explicitly, the normalized diffusion coefficients are systematically smaller for N_2 compared to that of CO_2, indicating that the particle fillers exert stronger influence upon the diffusion of N_2 molecules. Moreover, the quantitative influence of the filler particles is seen to depend explicitly on the temperature of interest. Both the preceding trends contrast with continuum mechanical theories in which the influence of particle fillers upon penetrant diffusivities is predicted to be of the form

$$\frac{D}{D_0} = \frac{1-\varphi}{1+\varphi/2} \quad (1)$$

where D_0 denotes the penetrant diffusivity in the pure polymer matrix and ϕ represents the volume fraction of the particle fillers. In other words, the diffusivity values normalized by the respective values in the pure polymer matrix, are predicted to follow a universal trend which depends only on the particle loading. In contrast, the results of Figure 8 indicates D/D_0 to be dependent on the identity of the penetrant and temperature. In the following, we present a discussion of the possible mechanisms underlying such trends.

dx.doi.org/10.1021/jp209294t |J. Phys. Chem. B 2012, 116, 95–103

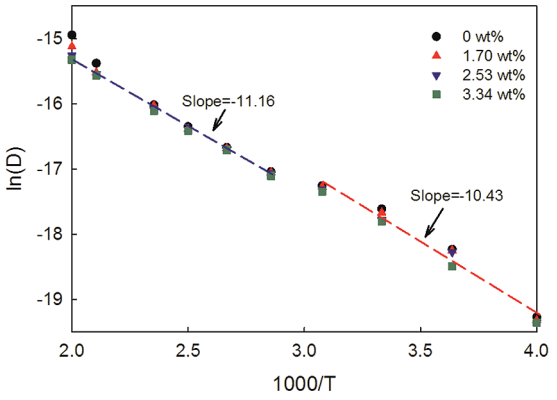

Figure 7. Arrhenius plot of diffusion of CO_2.

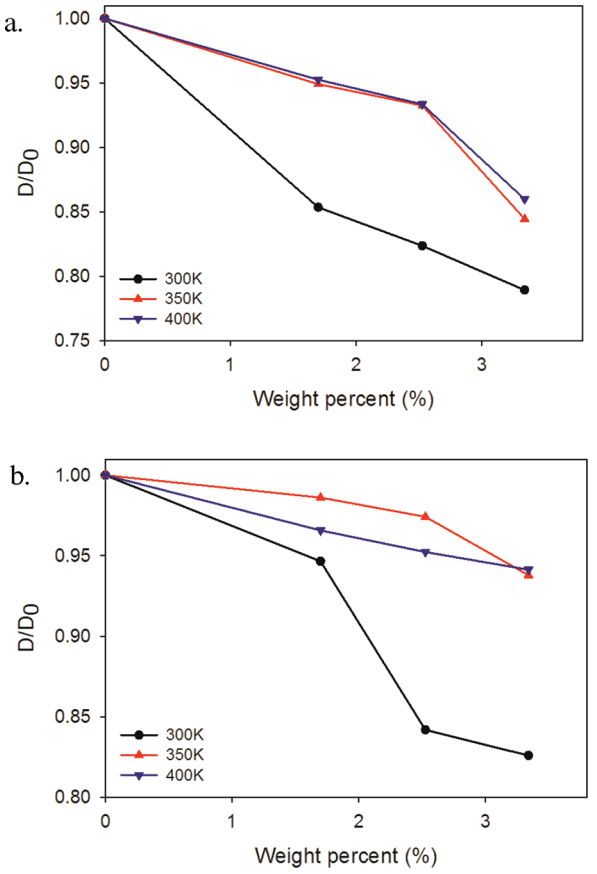

Figure 8. Gas diffusivities at 300, 350, and 400 K for N_2 (a) and CO_2 (b) (normalized to the respective values in the pure polymer matrix).

E. Influence of Temperature and Nanoparticles upon Penetrant Diffusivities: Discussion. First, we address the differences in the magnitudes of the influence of the nanoparticles upon the diffusivities of CO_2 and N_2. We suggest that such trends can be rationalized by considering the specific interactions between the gaseous penetrant and the nanoparticles. Such differences are most clearly evident in the radial distribution functions displayed in Figure 9, where it is seen that CO_2 is depleted near the surface of the nanoparticles due to its unfavorable interactions with the latter. In contrast, N_2 is seen to exhibit an enhancement near the nanoparticle surface, which exemplifies

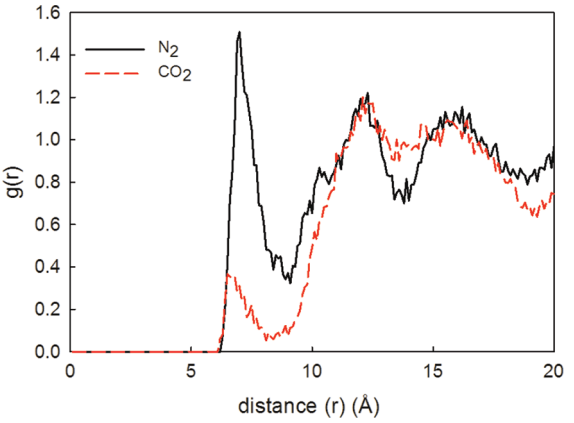

Figure 9. Radial distribution function $g(r)$ measured from center of nanoparticle for N_2 and CO_2 molecules.

the attractive interaction with latter. In this context it is evident that C_{60} nanoparticles present adsorbing surfaces for N_2 molecules and thereby further reduce the mobility (beyond the obstructional role of the particles) of the penetrants. In contrast, the C_{60} particles present repulsive surfaces for CO_2 molecules and therefore exhibit less influence upon the diffusion of the later.

To rationalize the temperature dependences noted in Figure 8, we invoke qualitative features of free volume theories of gas penetrant diffusion in glassy polymer matrices. In such models, the variations of the diffusivity of the penetrant D as a function of the temperature is expressed as a combination of two factors: (i) the probability of jumps of the penetrants in the matrix—a factor that is quantified through the relative ratios of the average free volume in the matrix to the critical free volumes required for the movement of the penetrant; (ii) an activation-energy term that quantifies the influence of the energy barrier the penetrant needs to overcome to execute the jumps in the polymer matrix.

Within the above picture, we hypothesize that the impact of the nanoparticles upon penetrant diffusivities can be divided into four components: (i) the obstructional character of the nanoparticles ("filler" effect) as quantified by eq 1 (however, while accounting for the penetrant particle interactions); (ii) nanoparticle-induced changes in the thermal expansion coefficient of the composite (such an effect would render the temperature dependence of the average free volumes to possess an explicit particle loading dependence and thereby endow the diffusivity to likewise be particle loading dependent); (iii) explicit impact of the nanoparticles upon the activation energy barrier for the penetrant transport in the polymer matrix (such a feature may arise if there are significant changes in the polymer structure at a scale which impacts the penetrant transport); (iv) effects arising from the interplay of polymer segmental dynamics and the filler role of the nanoparticles. As discussed in the Introduction, our earlier study on coarse-grained modeling of transport of penetrants demonstrated such effects to be important in the consideration of diffusion of larger probes.

Due to the lack of an accurate quantitative theory, it is difficult to directly extract the specific influence of the different factors above. As an alternative, we start with the simplest approach, viz., by assuming in a sequential manner that factors (i)−(iii) play a role, and discern if the simulation data can be rationalized on the basis of such contributions alone. In this context, the results displayed in Figure 8 already demonstrate that the temperature

dx.doi.org/10.1021/jp209294t |J. Phys. Chem. B 2012, 116, 95–103

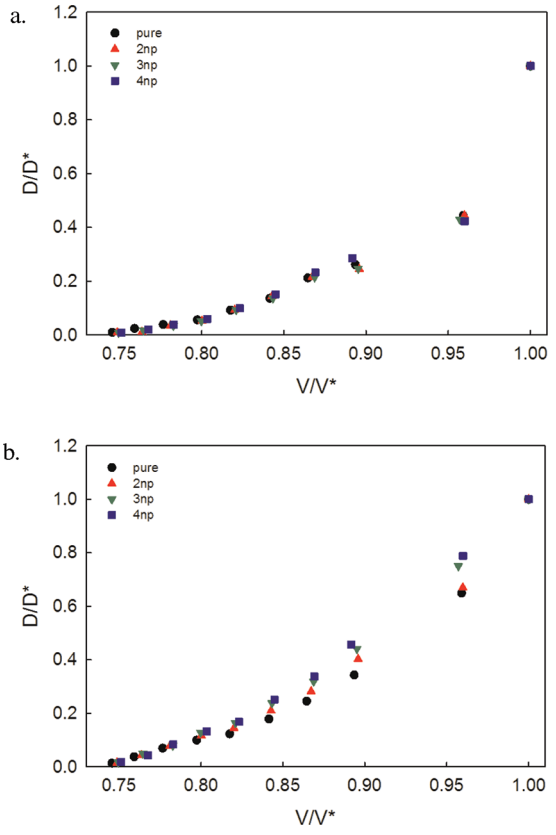

Figure 10. Normalized diffusivities plotted against normalized system volume for N_2 (a) and CO (b). D^* and V^* denote the diffusivities and systems volumes at 500 K and at the specified loading.

dependencies of the penetrant diffusivities cannot be rationalized as purely arising from effect (i). As a second step, we enquire if the differences in the thermal expansion of the matrix due to the incorporation of nanoparticles could rationalize the different temperature dependencies of the penetrant diffusivities. To probe this, we remove the "filler" effect by normalizing the diffusivity values D by its value at 500 K at the specified particle loading (Figure 10a,b). Subsequently, we compare the penetrant diffusivities expressed as this ratio to the thermal expansion of the matrix (relative to the volume at 500 K) for the different particle loadings. It is seen that in the case of N_2 molecules, the different diffusivity values collapse onto a single universal curve in this representation. This suggests that for N_2 molecules, the temperature dependence of the diffusivities for the different particle loadings (*relative to the filler-effect-modified diffusivities at 500 K*) can be rationalized purely through the thermal expansion of the polymer matrix and the accompanying changes in the average free volumes.

In contrast to the behavior of N_2 molecules, it can be seen that the CO_2 molecules do not show such a universal trend—however, the trend toward universality becomes more reasonable at lower temperatures. These results suggest that the temperature dependence of the diffusivities of CO_2 molecules for the different particle loadings cannot be rationalized exclusively through the changes in the average free volumes arising from the thermal expansion of the polymer matrix.

We speculate the origin of the differences in the behaviors of CO_2 and N_2 be related to the fundamentally different behavior seen for the temperature dependence of the penetrant diffusivity of CO_2 in the pure matrix (Figure 7). To recall, we rationalized the trends in Figure 7 on the basis of the hypothesis that such differences arose due to the size of the molecules under consideration. Explicitly, the dynamics of larger molecules such as CO_2 (and molecules such as propane studied in other articles) was argued to be more influenced by the segmental dynamics of matrix chains and hence be correlated to the glass transition of the matrix. In contrast, the dynamics of small molecule gases such as N_2 are known to undergo a transition to a hopping mode of transport at a temperature well above the glass transition temperature of the matrix. In this context, it is useful to recall the pertinent results of our earlier study, which used coarse-grained simulations to demonstrate that in situations where there is a coupling between the segmental dynamics of the polymer and the penetrant motion, the addition particles can lead to nontrivial interplay between the filler effect and the dynamics of the matrix. Explicitly, it was shown that the impact of the filler depends explicitly on the ratio of the polymer segmental time scale (a function of the temperature) and the penetrant diffusivity. In the present work, we borrow the findings of our earlier work and tentatively rationalize the trends seen in the behavior seen for CO_2 molecules at different temperatures to be a result of an interplay between the polymer segmental dynamics and the filler effect. At very low temperatures, the matrix chains become effectively frozen, and hence the diffusion of CO_2 resembles that of N_2.

IV. CONCLUSIONS

In this study we have used computer simulations to calculate the diffusivity of gas molecules through a polymer matrix with embedded nanoparticles at conditions above and below the glass transition temperature. The gas molecule was determined to diffuse through the simulation box in a hopping motion, which is consistent with a number of previous simulation studies on small penetrant diffusion in a glassy polymer. It was found that the addition of fullerene nanoparticles reduced the diffusion rate of the penetrants at all temperatures. We attributed the influence of nanoparticles as arising from a combination of three effects: (1) the obstructive nature of the nanoparticles; (2) changes in the thermal expansion coefficient due to the addition of the nanoparticles; (3) the interplay of polymer segmental dynamics and the filler role of the nanoparticles, and presented qualitative arguments to support our hypothesis.

■ ACKNOWLEDGMENT

This work was supported in part by a grant from Robert A. Welch Foundation (Grant F1599), the U.S. Army Research Office under grant W911NF-07-1-0268 and National Science Foundation (DMR 1005739). We acknowledge the Texas Advanced Computing Center (TACC) at The University of Texas at Austin for providing computing resources that have contributed to the research results reported within this paper. We thank Prof. David Brown for useful comments on the implementation of TEKMC scheme.

■ REFERENCES

(1) Persico, P.; Ambrogi, V.; Carfagna, C.; Cerruti, P.; Ferrocino, I.; Mauriello, G. *Polym. Eng. Sci.* **2009**, *49*, 1447.
(2) Wyser, Y.; Lange, J. *Packag. Technol. Sci.* **2003**, *16*, 149.

(3) Lagaron, J. M.; Cabedo, L.; Cava, D.; Feijoo, J. L.; Gavara, R.; Gimenez, E. *Food Addit. Contam.* **2005**, *22*, 994.
(4) Rhim, J. W. *Food Sci. Biotechnol.* **2007**, *16*, 691.
(5) Marand, E.; Jeong, H. K.; Krych, W.; Ramanan, H.; Nair, S.; Tsapatsis, M. *Chem. Mater.* **2004**, *16*, 3838.
(6) Freeman, B. D.; Lin, H. Q.; Van Wagner, E.; Toy, L. G.; Gupta, R. P. *Science* **2006**, *311*, 639.
(7) Cassidy, P. E.; Rubal, M.; Wilkins, C. W.; Lansford, C.; Yamada, Y. *Polym. Adv. Technol.* **2008**, *19*, 1033.
(8) Vijay, Y. K.; Sharma, A.; Kumar, S.; Tripathi, B.; Singh, M. *Int. J. Hydrogen Energy* **2009**, *34*, 3977.
(9) Okamoto, M. *J. Ind. Eng. Chem.* **2004**, *10*, 1156.
(10) Lin, C. W.; Chang, H. Y. *J. Membr. Sci.* **2003**, *218*, 295.
(11) Rhee, H. W.; Song, M. K.; Park, S. B.; Kim, Y. T.; Kim, K. H.; Min, S. K. *Electrochim. Acta* **2004**, *50*, 639.
(12) Sacca, A.; Carbone, A.; Passalacqua, E.; D'Epifanio, A.; Licoccia, S. Traversa, E.; Sala, E.; Traini, F.; Ornelas, R. *J. Power Sources* **2005**, *152*, 16.
(13) Krawiec, W.; Scanlon, L. G.; Fellner, J. P.; Vaia, R. A.; Giannelis, E. P. *J. Power Sources* **1995**, *54*, 310.
(14) Scrosati, B.; Croce, F.; Appetecchi, G. B.; Persi, L. *Nature* **1998**, *394*, 456.
(15) Scrosati, B. *Chem. Rec.* **2005**, *5*, 286.
(16) Yampol'skii, Y. P.; Pinnau, I.; Freeman, B. D. *Materials science of membranes for gas and vapor separation*; Wiley: Chichester, England; Hoboken, NJ, 2006.
(17) Bouma, R. H. B.; Checchetti, A.; Chidichimo, G.; Drioli, E. *J. Membr. Sci.* **1997**, *128*, 141.
(18) Merkel, T. C.; Freeman, B. D.; Spontak, R. J.; He, Z.; Pinnau, I.; Meakin, P.; Hill, A. J. *Science* **2002**, *296*, 519.
(19) Kang, Y. S.; Kang, S. W.; Kim, H.; Kim, J. H.; Won, J.; Kim, C. K.; Char, K. *Adv. Mater.* **2007**, *19*, 475.
(20) Choy, T. C. *Effective medium theory: principles and applications*; Clarendon Press; Oxford University Press: Oxford, England; New York, 1999.
(21) Jeffrey, D. J. *Proc. R. Soc. London Ser. a-Math. Phys. Eng. Sci.* **1973**, *335*, 355.
(22) Batchelo, Gk. *Annu. Rev. Fluid Mech.* **1974**, *6*, 227.
(23) Przyluski, J.; Siekierski, M.; Wieczorek, W. *Electrochim. Acta* **1995**, *40*, 2101.
(24) Fredrickson, G. H.; Bicerano, J. *J. Chem. Phys.* **1999**, *110*, 2181.
(25) Broutman, L. J.; Agarwal, B. D. *Polym. Eng. Sci.* **1974**, *14*, 581.
(26) Koros, W. J.; Moore, T. T.; Mahajan, R.; Vu, D. Q. *AIChE J.* **2004**, *50*, 311.
(27) Odegard, G. M.; Clancy, T. C.; Gates, T. S. *Polymer* **2005**, *46*, 553.
(28) Xue, L. P.; Borodin, O.; Smith, G. D. *J. Membr. Sci.* **2006**, *286*, 293.
(29) Hill, R. J. *Ind. Eng. Chem. Res.* **2006**, *45*, 6890.
(30) Pryamitsyn, V.; Hanson, B.; Ganesan, V. *Macromolecules* **2011**, Article ASAP. DOI: 10.1021/ma201712j.
(31) Cabral, J. T.; Wong, H. C.; Sanz, A.; Douglas, J. F. *J. Mol. Liq.* **2010**, *153*, 79.
(32) Polotskaya, G. A.; Gladchenko, S. V.; Zgonnik, V. N. *J. Appl. Polym. Sci.* **2002**, *85*, 2946.
(33) Theodorou, D. N. *Chem. Eng. Sci.* **2007**, *62*, 5697.
(34) Han, J.; Boyd, R. H. *Polymer* **1996**, *37*, 1797.
(35) Sacristan, J.; Mijangos, C. *Macromolecules* **2010**, *43*, 7357.
(36) Mozaffari, F.; Eslami, H.; Moghadasi, J. *Polymer* **2010**, *51*, 300.
(37) Pavel, D.; Shanks, R. *Polymer* **2005**, *46*, 6135.
(38) Theodorou, D. N. *Mol. Phys.* **2004**, *102*, 147.
(39) Theodorou, D. N.; Terzis, A. F.; Stroeks, A. *Macromolecules* **2002**, *35*, 508.
(40) Greenfield, M. L.; Theodorou, D. N. *Macromolecules* **2001**, *34*, 8541.
(41) Theodorou, D. N.; Karayiannis, N. C.; Mavrantzas, V. G. *Chem. Eng. Sci.* **2001**, *56*, 2789.
(42) Gusev, A. A.; Arizzi, S.; Suter, U. W.; Moll, D. J. *J. Chem. Phys.* **1993**, *99*, 2221.
(43) Gusev, A. A.; Suter, U. W. *J. Chem. Phys.* **1993**, *99*, 2228.
(44) Neyertz, S.; Brown, D. *Macromolecules* **2010**, *43*, 9210.
(45) Neyertz, S.; Brown, D.; Pandiyan, S.; van der Vegt, N. F. A. *Macromolecules* **2010**, *43*, 7813.
(46) Plimpton, S. *J. Comput. Phys.* **1995**, *117*, 1.
(47) Nose, S. *J. Chem. Phys.* **1984**, *81*, 511.
(48) Hoover, W. G. *Phys. Rev. A* **1985**, *31*, 1695.
(49) Andersen, H. C. *J. Chem. Phys.* **1980**, *72*, 2384.
(50) Siepmann, J. I.; Wick, C. D.; Martin, M. G. *J. Phys. Chem. B* **2000**, *104*, 8008.
(51) Siepmann, J. I.; Potoff, J. J. *AIChE J.* **2001**, *47*, 1676.
(52) Mayo, S. L.; Olafson, B. D.; Goddard, W. A. *J. Phys. Chem.* **1990**, *94*, 8897.
(53) Allen, M. P.; Tildesley, D. J. *Computer Simulation of Liquids*; Oxford University Press: New York, 1987.
(54)
(55) Rein, D. H.; Baddour, R. F.; Cohen, R. E. *J. Appl. Polym. Sci.* **1992**, *45*, 1223.
(56) Kropka, J. M.; Pryamitsyn, V.; Ganesan, V. *Phys. Rev. Lett.* **2008**, 101.
(57) Hofmann, D.; Fritz, L.; Ulbrich, J.; Schepers, C.; Bohning, M. *Macromol. Theory Simul.* **2000**, *9*, 293.
(58) Tocci, E.; Hofmann, D.; Paul, D.; Russo, N.; Drioli, E. *Polymer* **2001**, *42*, 521.
(59) Gee, R. H.; Boyd, R. H. *Polymer* **1995**, *36*, 1435.
(60) Pant, P. V. K.; Boyd, R. H. *Macromolecules* **1993**, *26*, 679.
(61) van der Vegt, N. F. A. *Macromolecules* **2000**, *33*, 3153.